

Understanding the Mechanical Properties of Self-Expandable Stents: A Key to Successful Product Development

Daisuke Yoshino* - Katsumi Inoue - Yukihito Narita
Tohoku University, Department of Mechanical Systems and Design, Japan

A medical device of mesh-shaped tubular structure called stent is frequently used to expand the constriction of a blood vessel. The stent normally has the structure of longitudinal repetition of wavy wire parts and strut parts, and its mechanical properties such as bending flexibility and rigidity in radial direction mainly depend on the shape of wavy wire and construction of the strut. In the first stage of this paper, the mechanical properties of self-expandable stents are evaluated using a non-linear finite element method. The initial stent models are generated in a 3D-CAD system, and their expanded shapes are predicted first. They form the finite elements for the evaluation of the mechanical properties, then the influences of stent shape on the mechanical properties are computed and discussed. In the second stage, a basic method for the selection of a stent is proposed from a view point of mechanics. This enables us to select useful stents that are well adapted to a patient's condition, though medical examination is necessary.

© 2008 Journal of Mechanical Engineering. All rights reserved.

Keywords: self-expandable stents, modeling, 3D-CAD systems, finite element method, biomechanics

0 INTRODUCTION

A stent is a tubular medical implement used for the treatment of stenoses developed in arteries. If the endothelial cells of a blood vessel are damaged because of stimulus by hypertension, diabetes mellitus, etc., fat accumulates thickly onto vessel walls, eventually causing arteriosclerosis. A stent is used as a measure for less invasive treatment of vasoconstriction lesions of such arteriosclerosis obliterans. Stents are classified roughly into the following two types: a self-expandable stent, which is extended independently with the characteristic of shape memory alloys if released from a sheath; and a balloon-expandable stent with no inflation capability itself, but which is instead expanded using a balloon catheter. The stent used presently in many procedures is referred to as second-generation; it consists of multiple wavy wire parts having a linear structure made of a perforated raw material circle pipe and folded up along the axial direction, with several strut parts connecting the wire parts.

For stents used in most cases, their shape has been devised according to the experience of doctors and designers; the shape is subsequently revised based on evaluation of mechanical property and clinical trials using prototypes. However, such a procedure requires much time, and presents

difficulties in quantitative evaluation of shape modification. Among many studies of stents that have been undertaken from a clinical perspective (for example, [1]), only a few have evaluated them based on their mechanical properties.

Schmitz et al. [2] summarized the measurement of the most relevant mechanical and dimensional parameters for a given stent design. They measured longitudinal flexibility, radial stiffness, foreshortening due to expansion and so on. Duda et al.[3] listed weight, radial rigidity, insertion property into the body, and radiolucency as mechanical characteristics that must necessarily be evaluated for a stent. They further proposed an evaluation method and evaluated characteristics of commercially available stents. Mori et al.[4] conducted four-point bending tests of stainless steel stents, then obtained flexural rigidity data and investigated buckling mode in various structures. Whitcher [5] computed the stress state in a stent and proposed a procedure for its use for fatigue fracture prediction. Several studies of stent materials were also reported (for example, [6]). Some recent studies have replaced prototype experiments with those using finite element analysis, although those studies were intended only for evaluation of mechanical properties of a stent (for example, [7], [8], [9] and [10]).

*Corr. Author's Address: Tohoku University, Department of Mechanical Systems and Design, 6-6-01, Aramaki-Aoba, Aoba, Sendai, Japan, yoshino@elm.mech.tohoku.ac.jp

Based on the experience in medical use, the stents are required to satisfy several clinical demands; they are a) scaffolding property, namely sufficient radial force to ensure vessel patency, b) conform smoothly to the anatomy and not injure the arterial wall, c) track-ability and push-ability to reach and cross target lesions, and d) small risk of restructure and occlusions in use. Demand a) relates to the rigidity in radial direction after expanding, and demands b) and c) can be realized in case the stent is flexible. Flexibility of stent mounted in a catheter also influences the demands c). Therefore, the stent should be just the right rigidity in radial direction to maintain enough blood stream without damaging the vessel wall, while it has to be as flexible as possible to fit various anatomical bends. The mechanical properties such as rigidity and flexibility are mainly determined by the shapes of wavy wire and strut. Demand d) is rather complicated, and the microscopic condition of blood stream may affect the restructure in use.

Nashihara [11] has developed a new self-expandable stent. It is called SENDAI stent after the name of city where he was studying. He drew a sketch of stent on a paper, and cut out the pattern to make a tubular paper model. It was bent or pressed to approximately estimate mechanical performances, then he modified the shape. Based on this trial and error experiments, he obtained a final shape. The biological effects of the SENDAI stent were examined in experiments with animals at Tohoku University School of Medicine, and it showed good effects available for clinical use.

Unfortunately, the rigidity in radial direction and flexibility of the SENDAI stent were not quantitatively estimated when Nashihara developed the stent. This means there is no clue to improve the mechanical properties. It is our ideal to develop and design such medical equipment adapted

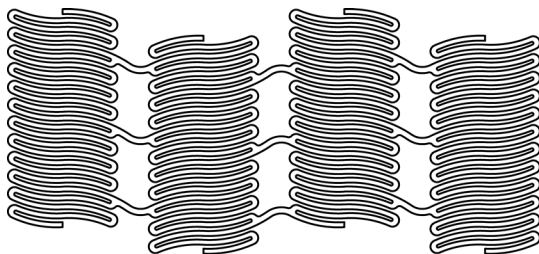


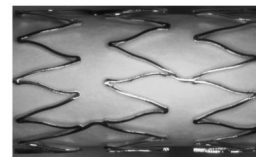
Fig. 1. Two-dimensional drawing of self-expandable SENDAI stent

precisely to each patient's symptoms and condition. The authors have studied design support systems and evaluation of mechanical properties of a stent, with the shape design of a self-expandable stent adapted to each patient's condition as the ultimate goal. A frame of computer-aided shape design support system has been presented using a 3D-CAD system and non-linear finite element method by Inoue et al. [12], then mechanical properties of the SENDAI stent is tried to evaluate by Inoue et al. [13].

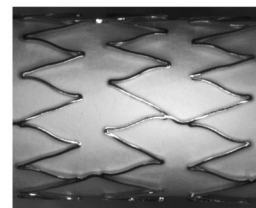
In this paper, the conception and functions of the design support system are reviewed first. A subsystem for the generation of two-dimensional (2D) shape of the stent is developed to flexibly modify the stent shape and it is implemented in the design support system. The shape of strut part of original SENDAI stent has been slightly modified to improve the push-ability of stent. The mechanical properties of both original and new SENDAI stents are evaluated in this paper to clarify the influence



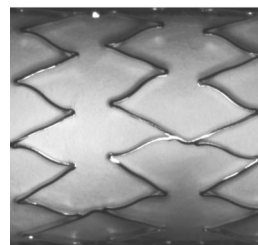
Initial stent $\phi 1.85$



$\phi 6.0$



$\phi 8.0$



$\phi 10.0$

Fig. 2. Photograph of SENDAI stents

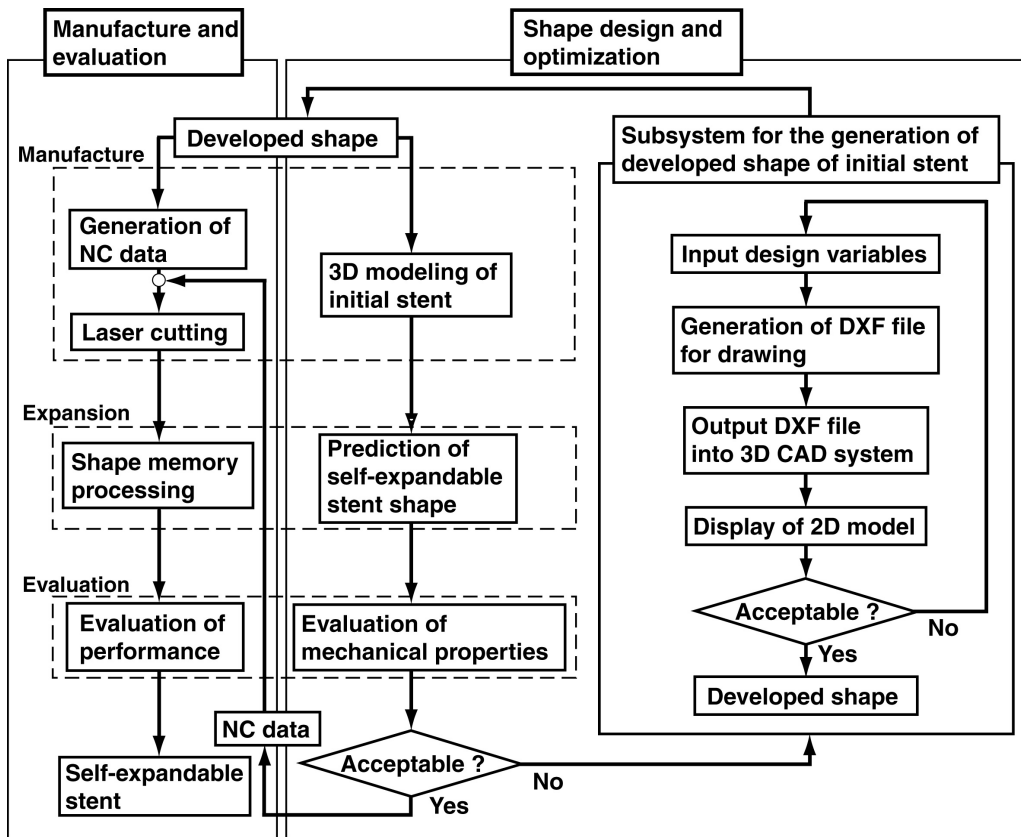


Fig. 3. Design support system for self-expandable stents

of stent shape on their mechanical properties; the estimation of the influence is very useful for the design modification of stents. Furthermore, based on the obtained mechanical properties, a method for the selection of a stent suitable to patient's condition is proposed from a view point of mechanics. A force generated at the end of stent in blood vessel, which is caused by the straightening of blood vessel, is also calculated from a simplified beam model and the influence of flexural rigidity of stent on the straightening is discussed.

1 MANUFACTURE PROCESS OF SENDAI STENT

The 2D drawing of SENDAI stent is illustrated in Figure 1. Every wire part consists of 12 pieces of wavy wire and the strut part connects them by 3 bridge wires. The stent is made of Nitinol tube of 1.85mm in diameter, 40-80mm long and about 0.25mm thick. Slits are processed on the tube by a laser beam then it is electrically polished. The stent finally has the structure of longitudinal

repetition of wavy wire parts and strut parts as shown in Figure 2. It is called initial stent in this paper. The initial stent is expanded step by step by repeating insertion of a thick rod and annealing. The shape-memory effect is expressed in this process. Stents with various diameters are also shown in Figure 2.

2 DESIGN SUPPORT SYSTEM FOR SELF-EXPANDABLE STENTS

2.1 Shape Design Support System

The design support system for self-expandable stents is shown in Figure 3. The left-hand side of Figure 3 shows manufacture and evaluation processes which are actually adopted in the production of SENDAI stent. As described above, the development, namely, 2D drawing of developed shape of stent is given first, and NC data are generated to cut a Nitinol tube by laser beam. The laser-processed tube is expanded step by step and heat treated. This is the shape memory processing. Expanded stents are bent and pressed

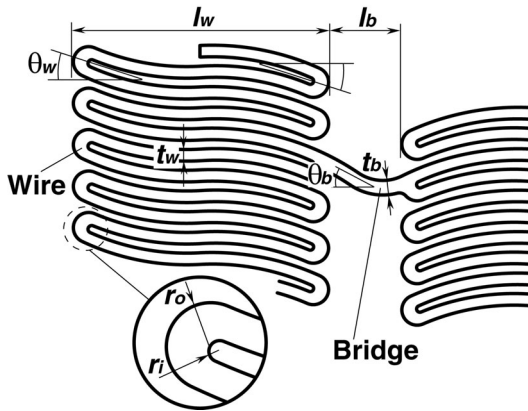


Fig. 4. Main design variables for SENDAI stent

to evaluate their performance in the next step, then the self-expandable stents are completed. Of course, the evaluation of performance is usually omitted after the trial manufacture is finished and the production of stents is made a good start.

The right-hand side of Figure 3 presents a flow chart of the shape design and optimization to be proposed. A three-dimensional (3D) stent shape corresponding to a laser-machined initial stent is formed first from 2D development of the stent of initial shape using 3D-CAD. Next, the 3D-CAD model is divided into finite elements, expansion analysis by the large deformation finite element method is conducted, and the expanded shape of the stent is predicted. Stiffness analysis is conducted using finite element method based on the predicted expansion model. Then mechanical properties of the stent are evaluated from the obtained result. These are respectively equivalent to the manufacturing process, expansion process, and evaluation process in actual fabrication.

NC data for processing are output to complete the processes after optimization by shape modification. Although processes subsequent to evaluation have not been completed at present, a 2D shape generation support subsystem that enables flexible alteration of a 2D development by changing the numerical value of design variables has been added to the original design support system [12]. This is useful also when creating 2D development at the first stage.

Details of the 2D shape generation support subsystem and the 3D modeling of initial stents are described later. Repeating the procedures described above, the evaluation of mechanical properties and the shape modification with the 2D shape generation support subsystem are considered

to allow design of a stent that is adapted to precise conditions of each patient.

2.2 Design Variables of SENDAI Stent

Design variables considered to influence the mechanical properties are set up for 2D development, as shown in Figure 4, where l_w and l_b respectively represent the axial lengths of wavy wire and bridge, θ_w and θ_b are angles to the axial direction, t_w and t_b respectively denote the widths of the linear elements of the wire and bridge, and r_i and r_o respectively signify the inside and outside diameters of the wire end. The wire part of the SENDAI stent is of a cyclic form in which 12 loose S-shapes were put in order; it consists of arcs. In drawing, l_w , θ_w , etc. are given, then the arc shape so that the linear elements continue is determined. The number of wires and bridges, represented respectively as n_w and n_b , and wall thickness t of the raw material tube are also used as design variables.

2.3 Subsystem for the Generation of Developed Shape of Initial Stents

At great effort, the conventional DXF file used for 2D development of a stent was put into 3D-CAD (SolidWorks) for shape modification. Therefore, a 2D shape generation support subsystem is developed as a prototype to modify the 2D development of a stent flexibly. First, an arc and a group of straight lines representing the stent shape are determined with the end point of the wire as the origin, based on numerical values of the given design variables. A DXF file, a CAD format file, is output after drawing them. Next, the 2D development of a stent of initial shape is generated by importing this DXF file into 3D-CAD.

The 2D shape generation support subsystem, which is constructed as a prototype, is implemented into a shape design support system, as shown in Figure 3, which has allowed enhanced efficiency of the stent shape design. In contrast to the conventional procedure using 3D-CAD, which required several hours for the shape change of a 2D development, this 2D shape generation support subsystem enables rapid shape change.

2.4 3D Modeling of Initial Stents

3D model of initial stent is formed from the 2D development of stent. This modeling is very

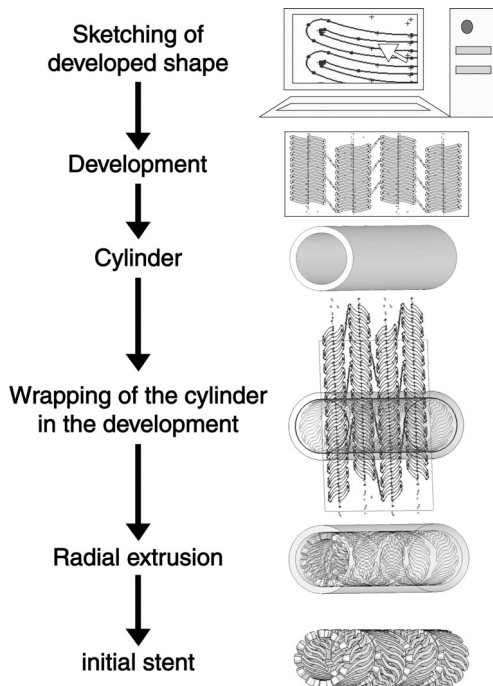


Fig. 5. Flow of modeling of initial stent in three-dimensional CAD system

important and complicated process. It depends on the functions of 3D-CAD system as well. The adopted flow of modeling is shown in Figure 5. The shape of stent is drawn on the surface of a tube using function of wrapping, then the initial stent model is generated on the tube by using the function of radial extrusion in a 3D-CAD system. Solid Works is used for this modeling. The solid models displayed at each process are also shown in the figure.

The CAD data of the initial stent are output using the data transformation format Parasolid and sent to the pre-processor of solver to generate the finite element mesh. This format is better than IGES format in our trial and we used MSC.Patran for this purpose. Then, it is expanded to a diameter of stent by non-linear finite element method in MSC.Marc.

3 PREDICTION OF EXPANDED SHAPE OF STENT

3.1 Analysis for Expanding Stent

Migliavacca et al. [14] conducted expansion and stress analyses of a balloon-expandable stent. However, no reports have described presumption

of the shape of self-expandable stents and analysis using an expansion estimation model, as far as the authors know.

In case of mounting a self-expandable stent in a thin sheath, or catheter, the stent is iced to shrink in diameter. It is inserted into a sheath in this condition; then the stent regains its initial shape by shape memory effect when it is released into a blood vessel. Therefore, the shrinkage and expansion in diameter should be reversible. The simulation described later estimates its mechanical properties at the expanded state and suggests shape modification for improving its mechanical properties. Subsequently, shrinking the modified shape indicates the final shape for laser processing. In addition, once the stent shape at the expanded state is obtained with sufficient precision by finite element analysis, the finite elements after deformation are useful also for simulation of mechanical properties. For those reasons, the prediction of the stent shape at the expanded state is of great importance.

This study uses the updated Lagrange method for formulation of a nonlinear equation, adopts the Newton-Raphson method for solution-seeking, and carries out elasto-plasticity analysis using the finite element method to estimate the expanded shape of a stent. The actual mechanical properties of a shape-memory alloy are known to vary according to heat treatment conditions. Because the heat treatment condition of the SENDAI stent has not been disclosed, the authors can not measure the property. So, the material properties are assumed to be those shown in Figure 6, with the stress-strain curve of a Ti-49.8Ni alloy processed at 500! subjected to the tensile test by Miyazaki et al. [15] being referred to. Its Young's modulus is 28 GPa, the Poisson's ratio is 0.3, and the initial yield stress is 140 MPa.

Expansion of stent is simulated as the forced displacement problem. The axial constraint is given at the wire ends as a boundary condition to avoid shortening of the stent length with forced radial displacement. Expansion analysis was conducted in this study starting from the initial shape with an external diameter of 1.85 mm, with the mesh regenerated when outside diameters of 4, 6, 8, and 10 mm were reached, for precision improvement, and for reduction of the time necessary for analysis. In addition, radial forced displacement was given as 100 increments in one expansion-analysis session.

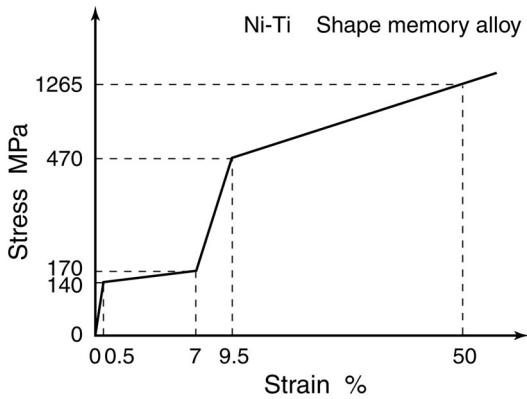


Fig. 6. Assumed stress-strain relationship for stent material

3.2 Prediction of Expanded Shape of SENDAI Stent

The two objects of analyses are the SENDAI-L80, the new model of SENDAI stent, and ST2621, the conventional model. Figure 7 illustrates their 2D development. Table 1 shows their typical design variables, which clearly reveal that the cyclic S-shapes of both wires are almost identical, but that a great difference pertains to their bridge part connecting wires. The ends of two adjacent wires are connected with a gap of two wire diameters in ST2621, although there is no gap in the SENDAI-L80.

The initial stent model of SENDAI-L80 with 6 wire parts and 5 strut parts is shown in Figure 8. 65,340 10-nodes tetrahedron elements are used for this modeling.

Figure 9 presents estimated results of expanded shapes of ST2621 with an external diameter of 4 mm and SENDAI-L80 of 8 mm, with comparison to real stents. Table 2 shows the estimated errors of expanded shapes. Because wire

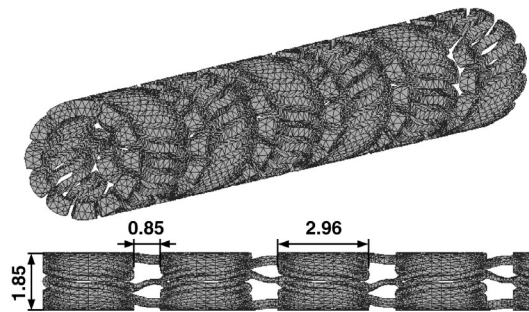


Fig. 8. Initial stent of SENDAI-L80 divided into 65,340 finite elements

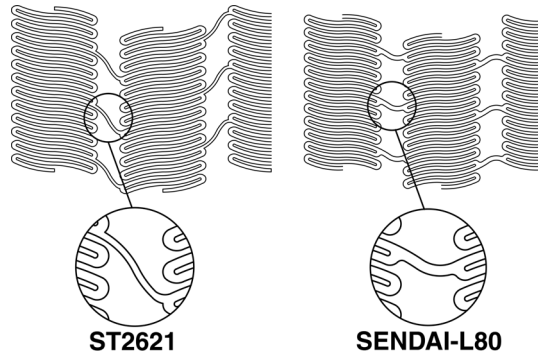


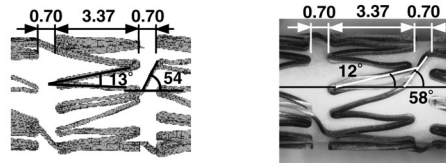
Fig. 7. Difference of bridge part between SENDAI-L80 and ST2621

Table 1. Design variables of ST2621 and SENDAI-L80

Design variables	ST2621	SENDAI-L80
Number of wires, n_w	12	12
Number of bridges, n_b	3	3
Wire length, l_w [mm]	3.37	2.96
Bridge length, l_b [mm]	0.88	0.85
Wire angle, θ_w [deg.]	22.8	24.4
Bridge angle, θ_b [deg.]	53.5	25.0
Wire width, t_w [mm]	0.14	0.14
Bridge width, t_b [mm]	0.11	0.17

length l_w and bridge length l_b are constraints, no shape error is considered for these. However, a difference occurs in the circumferential gap of wire ends in ST2621; the wire part is expanded linearly compared to that of a real stent in SENDAI-L80. Nevertheless, the shape error to the real stent does

Type : ST2621 ($\phi 4$)



Type : SENDAI-L80 ($\phi 8$)

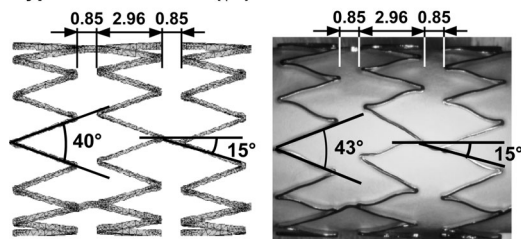


Fig. 9. Estimated results of expanded shapes, with comparison to real SENDAI stents

Table 2. Error of simulated shapes

Stent		θ_w [%]	θ_b [%]
ST2621	$\phi 4$	8	7
SENDAI-L80	$\phi 6$	0	0
	$\phi 8$	7	0
	$\phi 10$	4	0

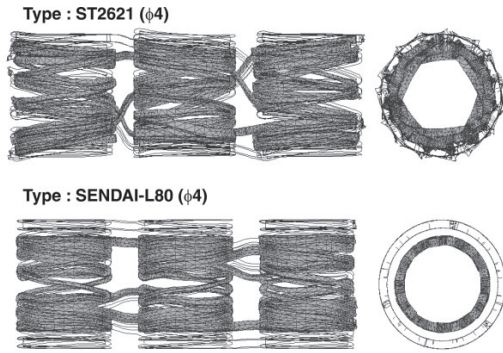


Fig. 10. Deformation of stents due to uniform radial pressure

not exceed 8 %, as shown in Table 2. Therefore, as described above, it is confirmed that this procedure can estimate the stent shape in the expanded state. The resultant expanded shape will be used for the model of evaluation of mechanical property.

4 EVALUATION OF MECHANICAL PROPERTIES OF STENTS

It is natural that a stent, as a product, has strain and stress states of its own depending on its manufacturing process. Nevertheless, it is not easy to measure them accurately. Assuming neither initial strain nor stress, the mechanical properties of a stent are evaluated.

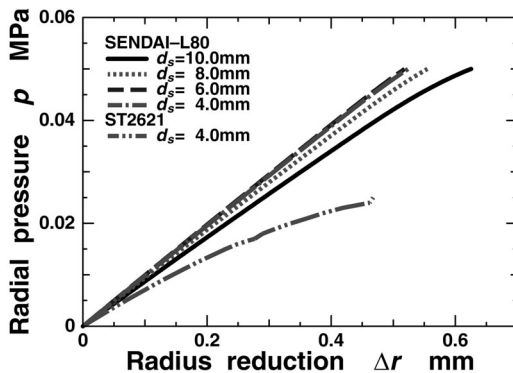


Fig. 11. Relation between radial pressure and radius reduction

4.1 Radial Stiffness

The center section of the stent is fixed in the axial and θ directions; radial pressure is applied to the outside of the stent elements. Then the compressive deformation of stent is analyzed. The state of deformation is shown in Figure 10. The SENDAI-L80 maintains a round shape and deformed almost uniformly, whereas the ST2621 shows greater deformation at the center than at both ends; it has no fair circular section.

Eight nodes at about equal intervals for one wire element are chosen; radius reductions at 96 points of 12 center wires are averaged to express the representative radius reduction. The relationship of the obtained stent radius reduction to pressure is presented in Figure 11.

The ratio of radial pressure applied to the outside surface of a stent p to radius reduction of the stent Δr defines the stiffness in the radial direction of a stent K_p as:

$$K_p = \frac{p}{\Delta r} \quad (1)$$

the relationship between radial stiffness obtained using Eq. (1) and the stent diameter is shown in Figure 12, which indicates that radial stiffness falls as the pressure increases in both stents. This decrease is attributable to the nonlinearity of radius reduction shown in Figure 11, which appears clearly in the stiffness drop of ST2621.

The radial stiffness of the SENDAI-L80 is greater than that of ST2621. Radial pressure engenders hoop stress in the stent. The decreased stent diameter is considered to occur because this hoop stress folds up the wire part and decreases

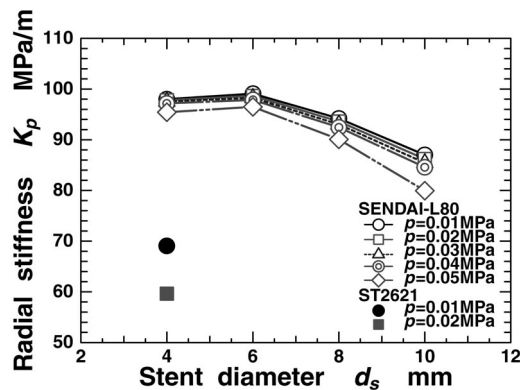


Fig. 12. Relation between radial stiffness and stent diameter

the angle of the aperture at the wire end. In the SENDAI-L80 with short wire length l_w , the force applied to a wire part decreases, so that the effectiveness to reduce the angle of aperture at the wire ends decreases. This decrease is inferred to suppress an increase in the radius reduction and has contributed to the rigidity improvement of SENDAI-L80. The above consideration has revealed that the wire length l_w affects the radial stiffness of a stent.

4.2 Flexural Rigidity

The left end of a stent is fixed, and the axial nodal force equivalent to the bending moment is applied to 12 nodes at the wire ends in the right end of the stent. This distributed load is given as divided into 100 increments, and bending deformation is analyzed. The shape after analysis is shown in Figure 13. Both ST2621 and SENDAI-L80 demonstrate great bending at the bridge part. The relationship between the obtained bending moment and curvature is presented in Figure 14.

Unnatural increase of bending moment is observed at $1/\rho = 0.025$ of SENDAI-L80 $d_s = 10$ mm. It is caused by the contact of wire ends of adjacent wire parts at the compression side of stent. This is unfavourable property for clinical use, and

an improvement should be considered. Numerical analyses and experiences suggest that the placement of adjacent wire parts, namely, the angle of bridge element θ_b , considerably influences on avoiding the contact of wire ends.

The following equation defines the flexural rigidity of a stent K_b :

$$K_b = \frac{M}{1/\rho} \quad (2),$$

where the bending moment applied to the stent is M , and the radius of curvature of the central axis of the stent is ρ . The relationship between the flexural rigidity of a stent obtained by Eq. (2) and the stent diameter is shown in Figure 15, which suggests that the flexural rigidity changes as the curvature changes in both stents. This relation originates in the nonlinearity of the relation between the bending moment and curvature, as shown in Figure 14. Obviously, the increase of flexural rigidity at $d_s = 10$ mm and larger curvature is caused by the contact of wire ends, as discussed above.

The flexural rigidity of SENDAI-L80 is greater than that of ST2621. Deformation of the bridge part is observed as a factor influencing flexural rigidity. The angle between end surfaces of adjacent wire parts of stents subjected bending moment is defined as the bending angle ϕ_b ; its relationship to the stent diameter is shown in Figure 16, which indicates that the bending angle of ST2621 is always greater than that of SENDAI-L80 for every stent diameter when the bending moment is constant. The reduction of the angle of a bridge element θ_b decreases the element length; consequently, it improves the flexural rigidity of a stent. Furthermore, the width of the bridge part t_b of the SENDAI-L80 is greater than that of the ST2621, which also enhances flexural rigidity. The above consideration has revealed that the width of a bridge part t_b and the angle of a bridge element θ_b strongly affect the flexural rigidity of a stent.

4.3 Influence of Shear Deformation on Flexural Rigidity

The load normal to the stent axis causes bending deflection as well as shear deformation in a stent. One end of a stent is fixed, and deflection including the shear deflection is evaluated on the conditions that apply nodal forces in the vertical

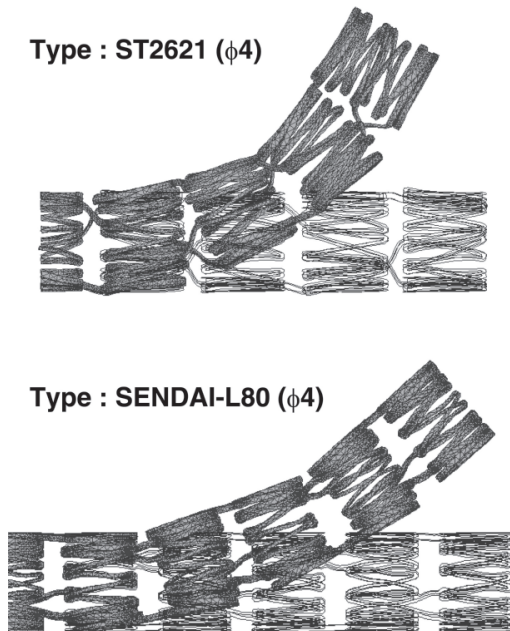


Fig. 13. Deflection of stents due to bending moment

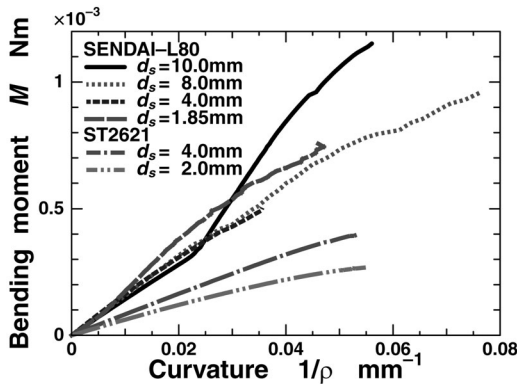


Fig. 14. Relation between bending moment and curvature

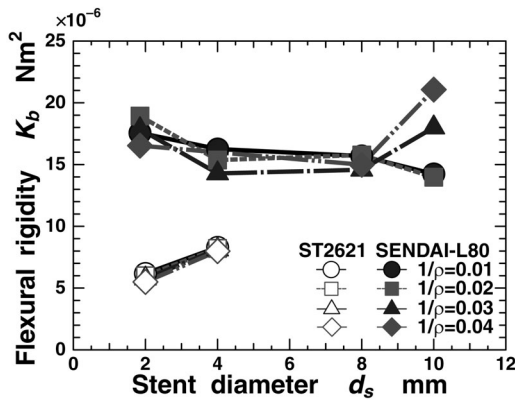


Fig. 15. Relation between flexural rigidity and stent diameter

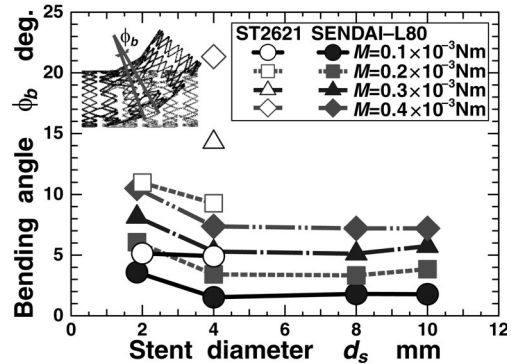


Fig. 16. Bending angle between end surfaces of adjacent wire parts of stents subjected bending moment

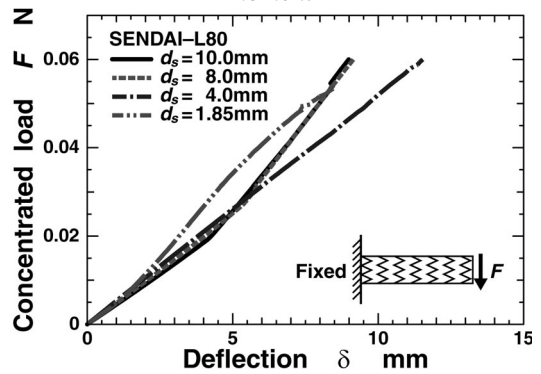


Fig. 17. Deflection at the loaded end of stent fixed at the other end

direction to 12 nodes at wire ends of the other end. This deflection is represented by δ . Figure 17 presents the obtained deflection δ at the center on the load surfaces. Deflection δ consists of bending deflection and shear deflection. Deflection with the additional constraint of revolution of a load surface to the same boundary condition as that above is estimated. The obtained deflection is regarded as shear deflection, and is expressed as δ_{shear} . Deflection incorporating only the deformation by bending $\delta_{bending}$ is obtainable from the following equation using deflection δ and shear deflection δ_{shear} :

$$\delta_{bending} = \delta - \delta_{shear} \quad (3).$$

The relationship of the obtained bending deflection, shear deflection and stent diameter is shown in Figure 18. The obtained deflection is normalized with flexural rigidity EI , where E is the elastic modulus of stent material, and I is the moment of inertia of cross sectional area of stent. The flexural rigidity is computed from Figure 14

using the obtained $\delta_{bending}$. Figure 18 demonstrates that shear deflection increases with the increase of stent diameter and applied load. Large ratio of initial stent is caused by small bending deflection. Shear deflection occupies 23-45 % of the bending deflection for every stent diameter, and the effect by shear becomes significant.

When placing a stent at the bend of a blood vessel, the blood vessel wall receives an intensive load from the stent end; in contrast, the stent receives an intensive load at its end. It is known as straightening of blood vessel, and it is discussed in detail later. Therefore, shear deformation of a stent cannot be disregarded.

5 SELECTION OF SUITABLE STENTS BASED ON MECHANICAL PROPERTIES

A stent should have sufficient stiffness for expansion of a narrowed section, and follow flexibly to a vessel wall. However, because neither patient conditions nor blood vessel shapes are

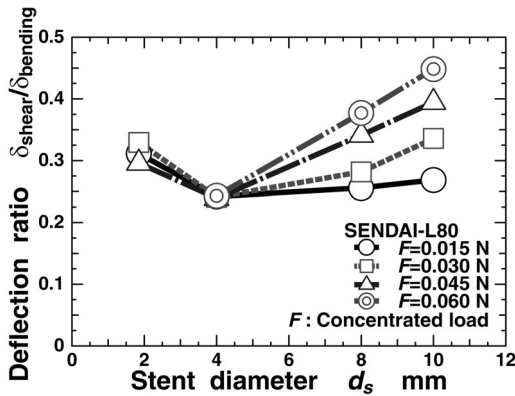


Fig. 18. Relation among bending deflection, shear deflection and stent diameter

identical, selection of a stent that is adequately adapted for each patient’s condition becomes important.

Selection and/or design of suitable stent depend a lot on the sense of a doctor and medical engineer. In this paper, for the purpose of design and manufacture of suitable stent for patient’s condition, the concept of selection is proposed in view of mechanics. The patient’s conditions, namely, a lesion of the stenosis, etc. as well as the diameter of blood vessel to secure blood stream are decided by a doctor. Referring to above-described information and analyzed mechanical properties, suitable stent diameter for securing blood stream is selected in the following section.

5.1 Estimation of Stiffness of Blood Vessel

To select a stent that is adapted precisely to a patient’s condition, it is necessary to estimate the stiffness of a blood vessel. The stiffness is clinically presented by the following equation using stiffness parameter β :

Table 3. Stiffness parameters of various arteries

No.	Artery	Stiffness parameter β
1	Femoral	11.2
2	Internal carotid	11.15
3	Common carotid	5.25
4	Vertebral(Intracranial)	15.82
5	Vertebral(Intracranial)	13.75
6	Vertebral(Extracranial)	7.58
7	RCA	36.3
8	LAD	50.8
9	LCCA	38.3

RCA, LAD and LCCA: right coronary, left anterior descending coronary and left circumflex coronary arteries

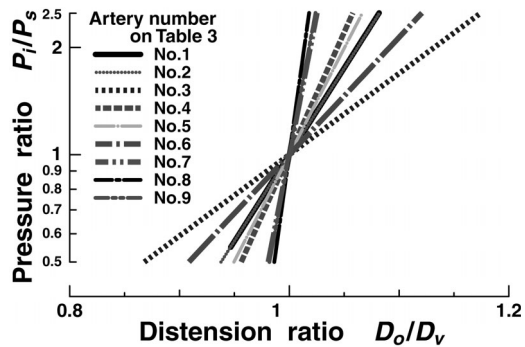


Fig. 19. Variation of diameter of human arteries due to internal pressure

$$\ln(P_i/P_s) = \beta \left(\frac{D_o}{D_v} - 1 \right) \quad (4)$$

where P_i represents internal pressure, P_s is the arbitrary reference internal pressure, D_o is the blood vessel outside diameter at loading P_i , and D_v is the blood vessel diameter at $P_i = P_s$. The above equation holds in the physiological blood pressure range. The stiffness parameter is easy to treat clinically because it is not influenced by internal pressure. The value of β depends on the part of blood vessels as shown in Table 3 (from [17] to [20]). Figure 19 indicates the relation between the pressure ratio P_i/P_s and distension ratio D_o/D_v obtained from Eq. (4). Although the stiffness of a vessel wall is presumed to increase by arteriosclerosis, negative results are also reported. Therefore this study assumes that the stiffness parameter is constant and uninfluenced by arteriosclerosis.

5.2 Determination of Stent Diameter and Rigidity in Radial Direction for Securing Blood Flow

Figure 20 presents the model of a narrowed section of blood vessel. D_v is the outside diameter of a blood vessel of normal state, t_v is the wall thickness, D_c and L_c are the diameter and length of a narrowed section, and D_r is the inside diameter after stent placement. The relationship between the internal pressure and the outside diameter of a femoral artery ($\beta = 11.2$) is obtained from Eq.(4) as shown in Figure 21, in which curves A-C indicate blood vessel characteristics of the narrowed state. Here we assume that the thickness of vessel $t_v = 1$ mm and narrowed diameter $D_c = 2$ mm is expanded to $D_r = 3.8$ mm near a normal state. The axis of

a little. As the reaction, the blood vessel is subjected to concentrated forces at the ends of stent in addition to the internal pressure required for expansion of the narrowed blood vessel, and as the result the vessel is somewhat straightened. This is called the straightening of blood vessel. Obviously the force due to straightening of blood vessel depends on the flexural rigidity of stent; the higher the flexural rigidity is, the larger the force acts. Too large force will damage the vessel wall, and in this sense, the straightening is an important measure for evaluating the performance of stents.

Although the straightening should be evaluated by precisely solving the deformation of

blood vessel combined with stent inside, it is considerably complicated problem. So, the force applied on a blood vessel at a stent end is estimated based on a simplified problem to confirm that it is not exceed the limit of force on the vessel wall.

A blood vessel and an inserted stent are modeled by a initially curved beam and a straight beam, respectively, and approximated by a statically indetermined beam as shown in Figure 23. Considering the symmetry, the beams are fixed at their center. Conditions required for this decision are the radius of blood vessel curvature at the narrow part ρ , inserted stent length L_s , the flexural rigidity of the stent $E_s I_s = k_b$, in addition to the blood vessel stiffness $E_v I_v = k_v$.

Initial deflection of the blood vessel in the state where no stent is inserted, δ_i , and deflections of the stent and blood vessel in the state where the stent is inserted, δ_s and δ_v , are given as the following equation:

$$\delta_i = \rho \left(1 - \cos \frac{L_s/2}{\rho} \right) \quad (6)$$

$$\delta_v = \frac{F(L_s/2)^3}{3E_v I_v} = \frac{F(L_s/2)^3}{3k_v} \quad (7)$$

$$\delta_s = \frac{F(L_s/2)^3}{3E_s I_s} = \frac{F(L_s/2)^3}{3k_b} \quad (8).$$

This is equal to the deflection of the stent when the stent is placed in a blood vessel. It gives:

$$\delta_s = \delta_i - \delta_v \quad (9).$$

Figure 24 shows the relation between concentrated load and deflection of SENDAI stent of $d_s = 4$ mm, which is selected in the preceding section, obtained from Figure 17. An end of stent is fixed and the force is applied at the free end. Marking the deflection $\delta = 4.5$ mm on the horizontal axis, the force acting on the vessel wall due to straightening is obtained from the intersecting point as $F = 0.024$ N as indicated in Figure 24. In case of the limit of force on the vessel wall $F_{limit} = 0.03$ N, the force due to straightening is smaller than the limit and the condition not to damage the vessel wall is confirmed. When we assume the limit of applied force F_{limit} which causes no damage to a blood vessel wall, the equation that the flexural rigidity of the stent should satisfy is derived as follows:

$$k_b \leq \frac{F_{limit} (L_s/2)^3}{3\delta_{bending}} \quad (10).$$

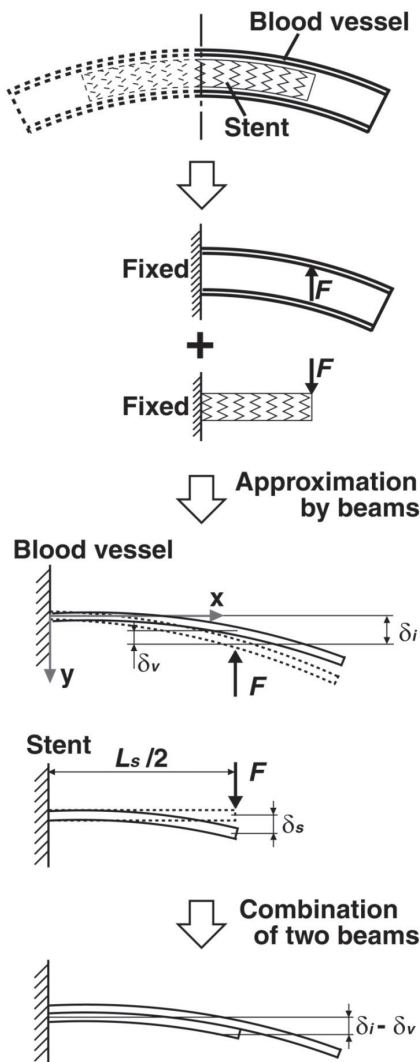


Fig. 23. Model of stent placement in curved blood vessel as a combined beam

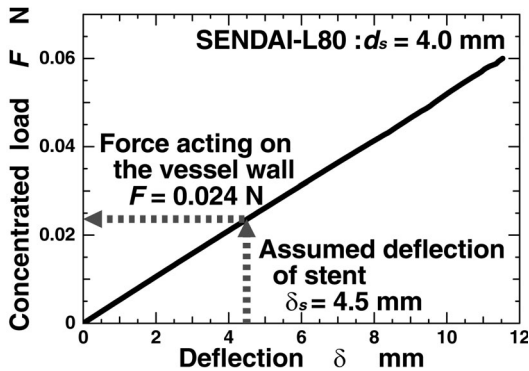


Fig. 24. Estimation of force acting on a vessel wall due to straightening

The flexural rigidity obtained from Eq. (10) may be used to roughly estimate whether the selection of stent is acceptable or not by comparing it with the flexural rigidity of existing stents evaluated in Chapter 4.

It is necessary to design a new stent that reduces its flexural rigidity with the application of mechanical property assessment considered in this paper when the limit of force applied to a blood vessel F_{limit} cannot be fulfilled with the existing mechanical properties.

6 DISCUSSION ON DESIGN AND SELECTION OF SUITABLE STENTS

Conventional design approaches accumulate improvements with design based on a designer's sense and evaluation of clinical trials to achieve a practical application. This system is trial-and-error-based design, which requires much time and labor to achieve improvement. It is therefore difficult to satisfy medical requirements. Correlation between medical requirements and mechanical properties must be clarified. The effect of design factors on mechanical properties must be evaluated quantitatively to reflect the medical requirements in a novel stent shape.

The design support system described in this paper can evaluate the effects of design factors on mechanical properties quantitatively as a routine flow. Presumption of extended shape and mechanical property evaluation with sufficient precision allows medical requirements to be reflected correctly in the stent shape. Furthermore, efficient shape design facilitates rapid shape change and improvement. For that reason, it is considered to contribute to reduction of working time and cost.

This paper does not step beyond suggesting a selection guideline with materials mechanics approximation. Establishment of a proper method of stent selection is anticipated, along with understanding the shape of the blood vessel containing the stent, the loaded condition, and the blood vessel based on more precise mechanical analysis. This enables the design of a stent that fits the symptoms of each patient. This is considered to bring about useful effects for the treatment of arteriosclerosis.

7 CONCLUSION

A shape design support system based on 3D-CAD and CAE was presented in this study, with the shape design of self-expanding stent adapted for a patient's condition as the final target. Using the functions of the system, a design method of the initial stent shape using this process, estimation of its expanded shape, assessment of its mechanical properties, and discussion of the influence of stent shape on those mechanical properties were conducted. In addition, a method of selecting a suitable stent to patient's conditions was proposed from a view point of mechanics. The results are summarized as follows.

1. A two-dimensional shape generation support subsystem was developed as a trial. The system sets up design variables of a stent and can modify its 2D development flexibly. This was embedded in a shape design support system. The efficiency of model production of the initial stent was enhanced.
2. Large deformation elasto-plasticity analysis with the finite element method can estimate the expanded shape of a stent with error of about 8 %.
3. Finite element analysis of a stent was conducted using the estimated expanded shape; mechanical properties were evaluated for two models of SENDAI stents: ST2621 and SENDAI-L80. The result with a new model SENDAI-L80 demonstrated greater flexural rigidity and radial stiffness.
4. Factors influencing mechanical properties were discussed from the difference in the shapes of ST2621 and SENDAI-L80. Results revealed that the width and angle of a bridge element affects flexural rigidity considerably, whereas the wire part length affects the radial stiffness.

5. Results showed the necessity of adopting flexural rigidity considering shear deflection as well as conventional bending deflection when a stent is placed at the bend of a blood vessel.
6. The characteristic of blood vessel was estimated from literatures, and the stent diameter to secure blood stream was selected based on the analyzed mechanical properties of stent.
7. The straightening of blood vessel was analyzed based on the simplified model of combined beams with the flexural rigidities of blood vessel and stent.
8. A method of selecting a suitable stent was proposed based on mechanical properties. It enabled selection of a stent that is well adapted to a patient's condition. In addition, the concept of design and manufacture of suitable stent for patient's condition was discussed for the future work.

8 REFERENCES

- [1] Nobuyoshi, M. *Frontiers in coronary stenting*. Nankodo, 1999 (in Japanese).
- [2] Schmitz, K.P., Behrend, D., Behrens, W., Schmidt, W. Comparative studies of different stent design. *Progress in Biomedical Research*, 1999, p. 52-58.
- [3] Duda, S.H., Wiskirchen, J., Tepe, G., Bitzer, M., Kaulich, T.W., Stoeckel, D., Claussen, C. Physical properties of endovascular stents: An experimental comparison. *Journal of Vascular and Interventional Radiology*, 2000, vol. 11, no. 5, p. 645-654.
- [4] Mori, K., Mitsudou, K., Iwata, H., Ikeuchi, K. Study on bending stiffness of stents. *Transactions of the Japan Society of Mechanical Engineers, Series C*, 2001, vol. 67, no. 662, p. 3078-3085 (in Japanese).
- [5] Whitcher, F.D. Simulation of IN VIVO loading conditions of nitinol vascular stent structures. *Computers & Structures*, 1997, vol. 64, no. 5/6, p. 1005-1011.
- [6] Igaki, K., Iwamoto, M., Yamane, H., Saito, K., Development of the novel biodegradable coronary stent (1st report, polyglycolic acid as the stent material). *Transaction of the Japan Society of Mechanical Engineers, Series A*, 1999, vol. 65, no. 639, p. 2379-2384 (in Japanese).
- [7] Takashima, K., Kitou, T., Mori, K., Ikeuchi, K. Simulation and experimental observation of contact conditions between stents and artery models. *Medical Engineering & Physics*, 2007, vol. 29, no. 3, p. 326-335.
- [8] Gay, M., Zhang, L., Liu, W. K. Stent modeling using immersed finite element method. *Computer Methods in Applied Mechanics and Engineering*, 2006, vol. 195, no. 33-36, 1, p. 4358-4370.
- [9] Wang, W.-Q., Liang, D.-K., Yang, D.-Z., Qi, M. Analysis of the transient expansion behavior and design optimization of coronary stents by finite element method. *Journal of Biomechanics*, 2006, vol. 39, no. 1, p. 21-32.
- [10] Lally, C., Dolan, F., Prendergast, P.J. Cardiovascular stent design and vessel stresses: a finite element analysis. *Journal of Biomechanics*, 2005, vol. 38, no. 8, p. 1574-1581.
- [11] Nashihara, H., Ishibashi, T. A possible product design for minute medical parts (Development of self-expanding stent made of memory alloy). *Journal of the Asian Design International Conference*, 2003, 1, CD-Rom.
- [12] Inoue, K., Matsuoka, T., Masuyama, T., Ito, T. A shape design support system for self-expandable stents. *Proceedings of the 15th International Conference on Engineering Design*, 2005, vol. 1, CD-Rom.
- [13] Inoue, K., Ito, T., Masuyama, T. Evaluation of mechanical properties of self-expandable stents. *Proceedings of the 5th International Conference on Advanced Engineering Design*, 2006, CD-Rom.
- [14] Migliavacca, F., Petrini, L. A predictive study of the mechanical behavior of coronary stents by computer modeling. *Medical Engineering & Physics*, 2005, vol. 27, no. 1, p. 13-18.
- [15] Miyazaki, S., Ohmi, Y., Otsuka, K., Suzuki, Y. Characteristics of deformation and transformation pseudoelasticity in Ti-Ni alloys. *Journal de Physique*, 1982, vol. 43, no. 12-Suppl., Colloque C4, p. 255-260.
- [16] Páczelt, I., Baksa, A., Szabó, T. Product design using a contact-optimization technique. *Journal of Mechanical Engineering – Strojniški vestnik*, 2007, vol. 53, no. 7-8, p. 442-461.

- [17] Hayashi, K., Handa, H., Nagasawa, S., Okumura, A., Moritake, K. Stiffness and elastic behavior of human intracranial and extracranial arteries. *Journal of Biomechanics*, 1980, vol. 13, no. 2, p. 175-184.
- [18] Hayashi, K., Nagasawa, S., Naruo, Y., Okumura, A., Moritake, K., Handa, H. Mechanical properties of human cerebral Arteries. *Biorheology*, 1980, vol. 17, no. 3, p. 211-218.
- [19] Hayashi, K., Nagasawa, S., Naruo, Y., Moritake, K., Okumura, A., Handa, H. Parametric description of mechanical behavior of arterial walls. *Proceedings of Japanese Society of Biorheology*, 1980, vol. 3, p. 75-78.
- [20] Igarashi, Y., Takamizawa, K., Hayashi, K., Ohnishi, K., Tanemoto, K. Mechanical properties of human coronary arteries. *Proceedings of Japanese Society of Biorheology*, 1983, vol. 6, p. 243-246.